Chemical Science

ROYAL SOCIETY OF CHEMISTRY

EDGE ARTICLE

View Article Online
View Journal | View Issue

Cite this: *Chem. Sci.*, 2024, **15**, 20013

All publication charges for this article have been paid for by the Royal Society of Chemistry

Received 10th August 2024
Accepted 1st November 2024

DOI: 10.1039/d4sc05375c

rsc.li/chemical-science

Pd(II)-catalyzed enantioselective C–H olefination and photoregulation of sterically hindered diarylethenes†

Guanlun Zhang,‡[a] Xu Wu,‡[b] Shiyu Mao,[b] Mengqi Li,*[a] Honglong Hu,[a] Bing-Feng Shi *[b] and Wei-Hong Zhu *[a]

Sterically hindered diarylethenes with intrinsic chirality have shown great potential in chiral signal regulation, light-controlled liquid crystals (LCs), *etc.* Their unique enantiospecific phototransformation between axial chirality of ring-open isomers and central chirality of ring-closed isomers can break through the bottleneck of interference between multiple chiral centers in traditional chiral diarylethenes. However, these intrinsic chiral diarylethenes require necessary chiral resolution through preparative chiral HPLC, typically resulting in limited separation efficiency and production scale. Here, we present an enantioselective olefination strategy to directly construct intrinsic chiral diarylethenes from a prochiral sterically hindered diarylethene, achieving high yields and enantioselectivity. The resulting isomers can be further decorated by incorporating mesogenic units, and the derivatives enable the successful reversible photoregulation of blue, green, and red reflection colors of LCs with excellent thermal stability, fatigue resistance, and little texture disorderliness, demonstrating the practical application potential of direct enantioselective olefination in photoregulation with intrinsic chiral diarylethenes.

Introduction

Diarylethene (DAE) is a kind of photoswitch that exhibits remarkable advantages including high thermal stability,[1] rapid response,[2] robust fatigue resistance,[3] *etc.*, attracting increasing attention in data storage,[4] light-controlled self-assembly,[5] super-resolution imaging,[6] and so on. Besides, chiral diarylethenes emerge as a compelling choice for chiral signal regulation,[7] light-controlled liquid crystal modulation,[8] *etc.* Traditionally, due to the small steric hindrance of ethene bridges, most diarylethenes exhibit racemic behavior resulting from the rapid rotation of side aryl groups, and extrinsic chiral groups are inevitable to induce a chiral preference for these diarylethenes, which will decrease the efficiency of chiral photoregulation because of the multiple chiral centers.[9] In recent years, we have developed an intrinsic chiral diarylethene by incorporating sterically hindered group benzobisthiadiazole as an ethene bridge and large bulky benzothiophene as side aryl groups. Complete inhibition of racemization and successful isolation of intrinsic chiral enantiomers were achieved.[10] The unique enantiospecific phototransformation between the axial chirality of the ring-open isomer and the central chirality of the ring-closed isomer can effectively avoid interference between multiple chiral centers in traditional chiral diarylethenes. However, this kind of diarylethene requires necessary chiral resolution through preparative chiral HPLC for application, typically accompanied by limited separation efficiency and production scale (Fig. 1a).

Asymmetric catalysis has been proven to be a promising strategy for efficiently synthesizing chiral molecules.[11] Besides, enantioselective C–H activation has emerged as a powerful strategy to construct biaryl atropisomers[12] in recent years, simply introducing chirality by one step. Motivated by this, we propose the asymmetrical synthesis of intrinsic chiral diarylethenes by enantioselective C–H activation, starting from prochiral diarylethene 4,5-bis(2,5-dimethylthien-3-yl)benzo[1,2-*c*:3,4-*c*′]bis([1,2,5]thiadiazole) (BTTE, **1a**)[13] with a sterically hindered ethene bridge (Fig. 1b). A series of sterically hindered intrinsic chiral diarylethenes have been constructed by enantioselective olefination with high yields and enantioselectivity, which can efficiently reduce the dependence on preparative chiral HPLC. Moreover, this strategy could achieve better accommodation and tolerance of the structures of diarylethenes

[a]*Key Laboratory for Advanced Material, Joint International Research Laboratory of Precision Chemistry and Molecular Engineering, Feringa Nobel Prize Scientist Joint Research Center, Shanghai Key Laboratory of Functional Materials Chemistry, Institute of Fine Chemicals, Frontiers Science Center for Materiobiology and Dynamic Chemistry, School of Chemistry and Molecular Engineering, East China University of Science & Technology, Shanghai 200237, China. E-mail: whzhu@ecust.edu.cn; mengqi15@126.com*

[b]*Department Center of Chemistry for Frontier Technologies, Department of Chemistry Zhejiang University, Hangzhou 310027, China. E-mail: bfshi@zju.edu.cn*

† Electronic supplementary information (ESI) available. CCDC 2359686 (**8**). For ESI and crystallographic data in CIF or other electronic format see DOI: https://doi.org/10.1039/d4sc05375c

‡ These authors contributed equally to this work.

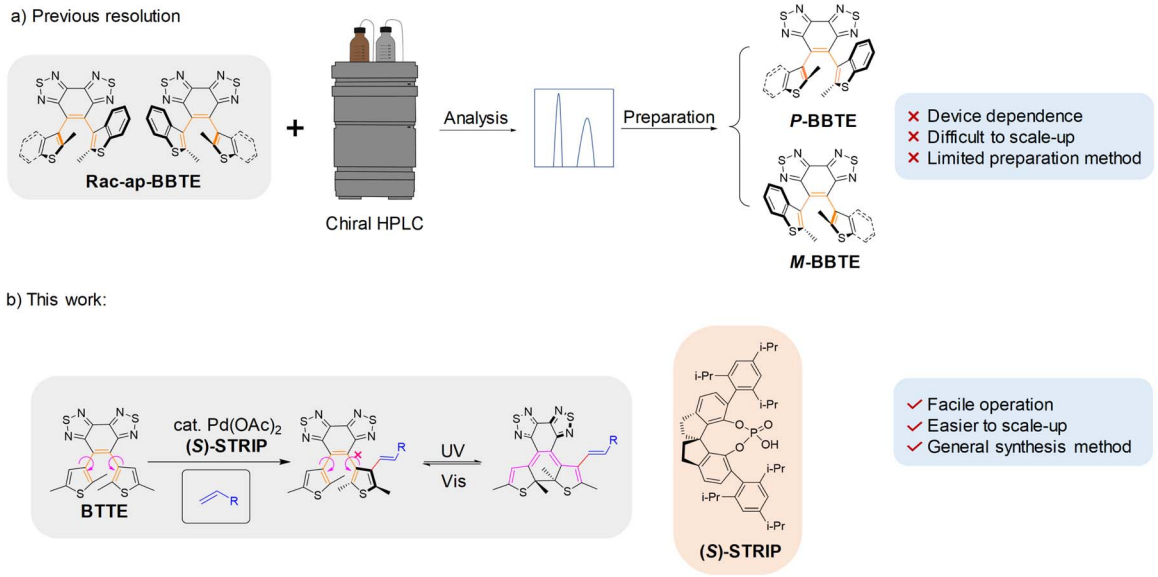

Fig. 1 Comparison between previous chiral resolution and direct enantioselective olefination. (a) Traditional chiral resolution process of the sterically hindered diarylethene 4,5-bis(2-methylbenzo[*b*]thien-3-yl)benzo[1,2-*c*:3,4-*c*′]bis([1,2,5]thiadiazole) (BBTE) by preparative chiral HPLC. (b) A novel strategy for the direct enantioselective olefination of sterically hindered diarylethenes with several advantages, such as facile operation, being easier to scale up, and a general synthesis method. Note: enantioselective olefination can increase the rotation barrier of side aryl groups of sterically hindered diarylethenes, resulting in the steady existence of their chiral enantiomers and achieving specific enantioselectivity at the same time, which can efficiently reduce the dependence on preparative chiral HPLC.

than the original chiral resolution. The resulting intrinsic chiral diarylethenes are further modified by incorporating mesogenic units, and subsequently, we embed these derived diarylethenes into a LC to photoregulate its helical superstructure. Precise photoregulation of blue, green, and red reflection colors of the LC has been achieved with good thermal stability, fatigue resistance, and little texture disorderliness, illustrating the practical application potential of direct enantioselective olefination in photoregulation with intrinsic chiral diarylethenes.

Results and discussion

Direct enantioselective olefination of sterically hindered diarylethene BTTE

According to our previous research, a large sterically hindered ethene bridge and β-substituted thiophene group with large bulk can significantly increase the rotation barrier and completely inhibit the axis's rotation of diarylethenes.[14] To further verify the impact of the benzothiadiazole ethene bridge, we calculated the rotation barrier of the parallel conformers of BTTE and a reference DAE (1,2-bis(2,5-dimethyl-3-thienyl) perfluorocyclopentene, **1b**) using M06-2X functional with a def2tzvp basis set (Table S2†).[15] The rotation barrier of BTTE (19.03 kcal mol^{-1}) is much higher than that of **1b** (5.10 kcal mol^{-1}), demonstrating that the benzothiadiazole ethene bridge can introduce large steric hindrance to the axis rotation in DAE. Based on the discussions above, it is possible to introduce chirality into prochiral sterically hindered diarylethene BTTE by enantioselective substitution of β-proton. In addition, the α-methyl group of thiophene in BTTE can avoid other possible reacting sites. Additionally, previous studies have demonstrated that benzothiadiazole can serve as an effective directing group (DG) for realizing C–H activation.[16] Thus, we believe that benzobisthiadiazole will have a similar ability. Hence, we decided to employ asymmetric C–H olefination, which has been proved to have good reactivity, enantioselectivity, and endurance of heteroatoms to introduce chirality into achiral BTTE.[17]

Optimizing reaction conditions

We first investigated the reaction of BTTE bearing a benzobisthiadiazole DG as the model substrate with phenyl acrylate (**2a**) as the olefination reagent. We have found that spiro phosphoric acids (SPAs) could enhance both the reactivity and enantioselectivity in Pd-catalyzed enantioselective synthesis of atropisomeric biaryl *via* asymmetry C–H activation.[18] Therefore, optimization was first done with a survey of chiral phosphoric acids, including spiro phosphoric acids (Table 1, entries 1–7) and BINOL-derived phosphoric acids (entries 8–10). The reactivity and enantioselectivity were sensitive to the steric environment of SPAs. (*S*)-STRIP **L2** bearing 2,4,6-tri-*iso*-propylphenyl gave the highest enantioselectivity (86.5 : 13.5 er) in 37% yield (entry 2) possibly because **L2** can impose more effective steric repulsion in the C–H activation process.[17a] The solvent effects were then examined (entries 11–17). The use of dibutyl ether may reduce the background reaction and lead to better enantiocontrol (96 : 4 er; entry 11), but with dramatically reduced yield (15%). Using trichloromethane as the solvent gave a high yield (80%) and poor enantiocontrol (80 : 20 er; entry 13) possibly due to better solubility of substrates. Then, further investigation of solvents revealed that a mixture containing

Table 1 Optimization of reaction conditions[a]

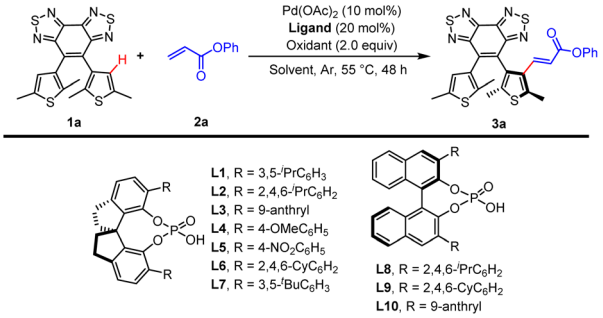

Entry	Ligand	Solvent	Oxidant	Yield[d] (%)	er[e]
1	**L1**	1,4-Dioxane	AgOAc	43	78 : 22
2	**L2**	1,4-Dioxane	AgOAc	37	86.5 : 13.5
3	**L3**	1,4-Dioxane	AgOAc	54	51 : 49
4	**L4**	1,4-Dioxane	AgOAc	50	51 : 49
5	**L5**	1,4-Dioxane	AgOAc	10	52 : 48
6	**L6**	1,4-Dioxane	AgOAc	53	68 : 32
7	**L7**	1,4-Dioxane	AgOAc	44	65 : 35
8	**L8**	1,4-Dioxane	AgOAc	64	68 : 32
9	**L9**	1,4-Dioxane	AgOAc	34	67 : 33
10	**L10**	1,4-Dioxane	AgOAc	54	51 : 49
11	**L2**	$^{n}Bu_2O$	AgOAc	15	96 : 4
12	**L8**	$^{n}Bu_2O$	AgOAc	62	84.5 : 15.5
13	**L2**	$CHCl_3$	AgOAc	72	80 : 20
14	**L8**	$CHCl_3$	AgOAc	79	85 : 15
15	**L2**	$CHCl_3$/$^{n}Bu_2O$ (1 : 1)	AgOAc	66	95 : 5
16	**L2**	*o*-DCB/$^{n}Bu_2O$ (1 : 1)	AgOAc	65	97 : 3
17	**L2**	$CHCl_3$/*o*-DCB/$^{n}Bu_2O$ (1 : 1 : 1)	AgOAc	78	95 : 5
18[b]	**L2**	$CHCl_3$/*o*-DCB/$^{n}Bu_2O$ (1 : 1 : 1)	AgOAc	50	94 : 6
19[c]	**L2**	$CHCl_3$/*o*-DCB/$^{n}Bu_2O$ (1 : 1 : 1)	AgOAc	85	95.5 : 4.5
20	**L8**	$CHCl_3$/*o*-DCB/$^{n}Bu_2O$ (1 : 1 : 1)	AgOAc	76	84.5 : 15.5
21	**L9**	$CHCl_3$/*o*-DCB/$^{n}Bu_2O$ (1 : 1 : 1)	AgOAc	14	95 : 5
22	**L2**	$CHCl_3$/*o*-DCB/$^{n}Bu_2O$ (1 : 1 : 1)	$Cu(OAc)_2$	11	94.5 : 5.5
23	**L2**	$CHCl_3$ *o*-DCB/$^{n}Bu_2O$ (1 : 1 : 1)	BQ	22	94 : 6

[a] Reaction conditions: **1a** (0.10 mmol), **2a** (0.15 mmol), $Pd(OAc)_2$ (10 mol%), **Ligand** (20 mol%), oxidant (2.0 equiv.) in solvent (2 mL), 55 °C, 48 h under Ar. [b] In air. [c] 60 h. [d] Isolated yield. [e] The er value was determined by chiral HPLC. *o*-DCB = 1,2-dichlorobenzene.

trichloromethane/1,2-dichlorobenzene/dibutyl ether (1 : 1 : 1, v/v/v) which could enhance the solubility of substrates and potentially inhibit the background reaction at the same time was optimal (78%, 95 : 5 er; entry 17). The yield could be improved to 85% with a slightly increased er value (95.5 : 4.5 er; entry 19) when the reaction time was prolonged to 60 h. The screening of oxidants demonstrated that AgOAc was superior for the transformation (entries 21–23 in Table 1; and entries 1–9 in Table S1†). Overall, the optimal reaction conditions were identified as the following: **1a** (0.1 mmol), **2a** (0.15 mmol), $Pd(OAc)_2$ (10 mol%), (*S*)-STRIP **L2** (20 mol%), AgOAc (2 equiv.) under Ar in trichloromethane/1,2-dichlorobenzene/dibutyl ether (1 : 1 : 1, v/v/v), 55 °C, 60 h.

Scope of the substrates

With the optimal reaction conditions in hand, we set out to explore the scope of this methodology concerning the olefin coupling partner (Scheme 1). Phenyl acrylates carrying various electron-withdrawing and -donating substituents at the *para*-position gave the desired products in moderate to high yields with good enantioselectivity (**3b–3g**, 43–88%, 93.5 : 6.5–95 : 5 er). Phenyl acrylates substituted at the *ortho*- or *meta*-position also reacted efficiently (**3h**, 57%, 94 : 6 er; **3i**, 67%, 88.5 : 11.5 er). It was worth mentioning that phenyl acrylates substituted with a halogen (**3d** and **3h**) and silicon (**3g**) were compatible with this reaction. Naphthyl acrylates also participated in the reaction effectively (**3j**, 68%, 95 : 5 er). Then we screened several generally available esters, such as *n*-butyl, *t*-butyl, methyl, ethyl, cyclohexyl, and benzyl, and all these acrylates proceeded smoothly to afford the desired products (**3k–3r**, 62–86%, 86.5 : 13.5–94 : 6 er; **3s**, 65%, $S_a : R_a$ = 88.5 : 11.5; **3t**, 55%, 88 : 12 er). α,β-Unsaturated ketone was used as the olefination reagent to provide the product in lower yield and enantioselectivity (**3u**, 48%, 87 : 13 er). To our delight, diethyl vinyl phosphonate also reacted effectively to give the desired product in good yield and enantioselectivity (**3v**, 74%, 93.5 : 6.5 er). Acrylamide also reacted

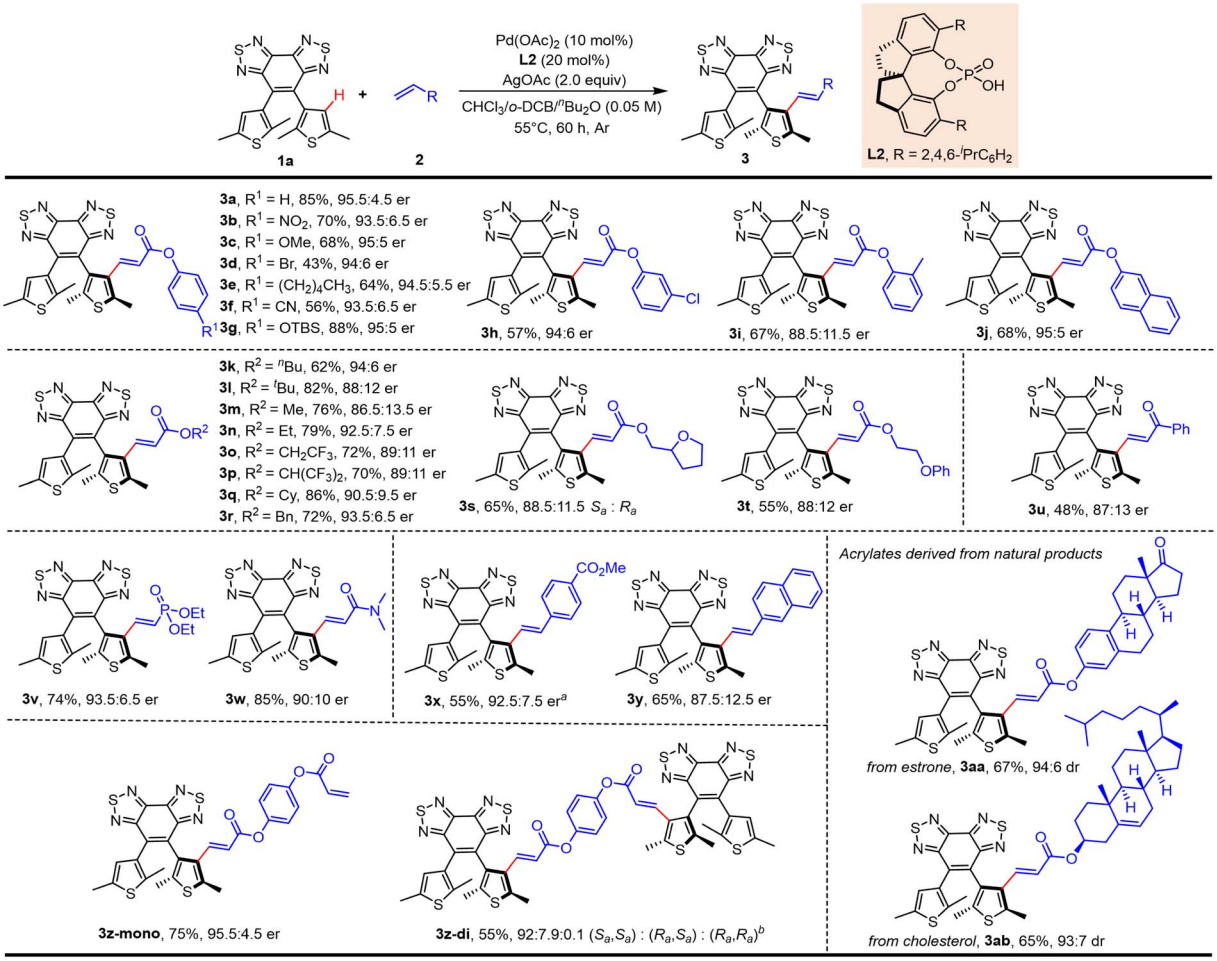

Scheme 1 Substrate scope. Reaction conditions: **1a** (0.10 mmol), **2** (0.15 mmol), $Pd(OAc)_2$ (10 mol%), **L2** (20 mol%), AgOAc (2.0 equiv.) in $CHCl_3$/1,2-dichlorobenzene/$^nBu_2O$ (1 : 1 : 1, 2 mL), 55 °C, 60 h under Ar. [a]In toluene/$^nBu_2O$ (1 : 1, 2 mL). [b]**1a** (0.30 mmol), **2a** (0.1 mmol), $Pd(OAc)_2$ (20 mol%), **L2** (40 mol%), AgOAc (4.0 equiv.) in $CHCl_3$/1,2-dichlorobenzene/$^nBu_2O$ (1 : 1 : 1, 2 mL).

smoothly, giving the alkenylation product in excellent yield and moderate er (**3w**, 85%, 90 : 10 er). Notably, aromatic alkenes, such as styrene and vinyl naphthalene, employed as coupling partners were well tolerated (**3x**, 55%, 92.5 : 7.5 er; **3y**, 65%, 87.5 : 12.5 er). To further demonstrate the utility of this protocol, we further examined the reaction with olefins derived from the core structures of natural products, affording the desired olefinated products in good yields and diastereoselectivity (estrone, **3aa**, 67%, 94 : 6 er; cholesterol, **3ab**, 65%, 93 : 7 er). To prove the practical potential of this strategy, scale-up synthesis and further transformations were conducted (Scheme 2). The olefination of **1a** with phenyl acrylate (**2a**) on a 2 mmol scale under the standard conditions gave the corresponding product in good yield without the loss of enantioselectivity (**3a**, 74%, 95.5 : 4.5 er). To further demonstrate the applicability of this strategy, the obtained diarylethene **3a** above was further decorated for LC photomanipulation. To enhance the miscibility and stability of the resulting chiral photoswitches in LC systems, a series of functional molecules were synthesized by introducing mesogenic units (green part in Scheme 2). This was expected to effectively reduce the disorderliness and deformation of LC induced by dopants and increase the photoregulatory ability of corresponding molecules.[19] In the presence of DIBAL-H, the ester group of **3a** could be selectively reduced to the allyl alcohol **4** (87%, 97 : 3 er), which could be then condensed with benzoic acid derivatives to obtain axially chiral ester **5** (93%, 96 : 4 er) with the retention of axial chirality. Treatment of **3a** with LiOH resulted in hydrolysis of the ester group to give carboxylic acid **6** (92%, 96 : 4 er) in a nearly quantitative yield without loss of enantioselectivity. Meanwhile, the oxidative cleavage of the double bond could be performed to aldehyde **7** (86%, 95 : 5 er) without notable change in enantioselectivity, and it could be readily transformed into the novel axially chiral carboxylic acid **8**, which is an essential prerequisite for further introducing mesogenic units. Then, we successfully developed a novel strategy for the effective synthesis of a series of axially chiral esters **9** (81%, 94 : 6 er), **10** (90%, 94.5 : 5.5 er), and **11** (78%, 94.5 : 5.5 er) in good yields and enantioselectivity *via* condensation of acid **8** with aliphatic or phenol derivatives containing mesogenic units as coupling partners to modify compatibility with the LC. Besides, the absolute configuration of **8** was determined as S_a by single

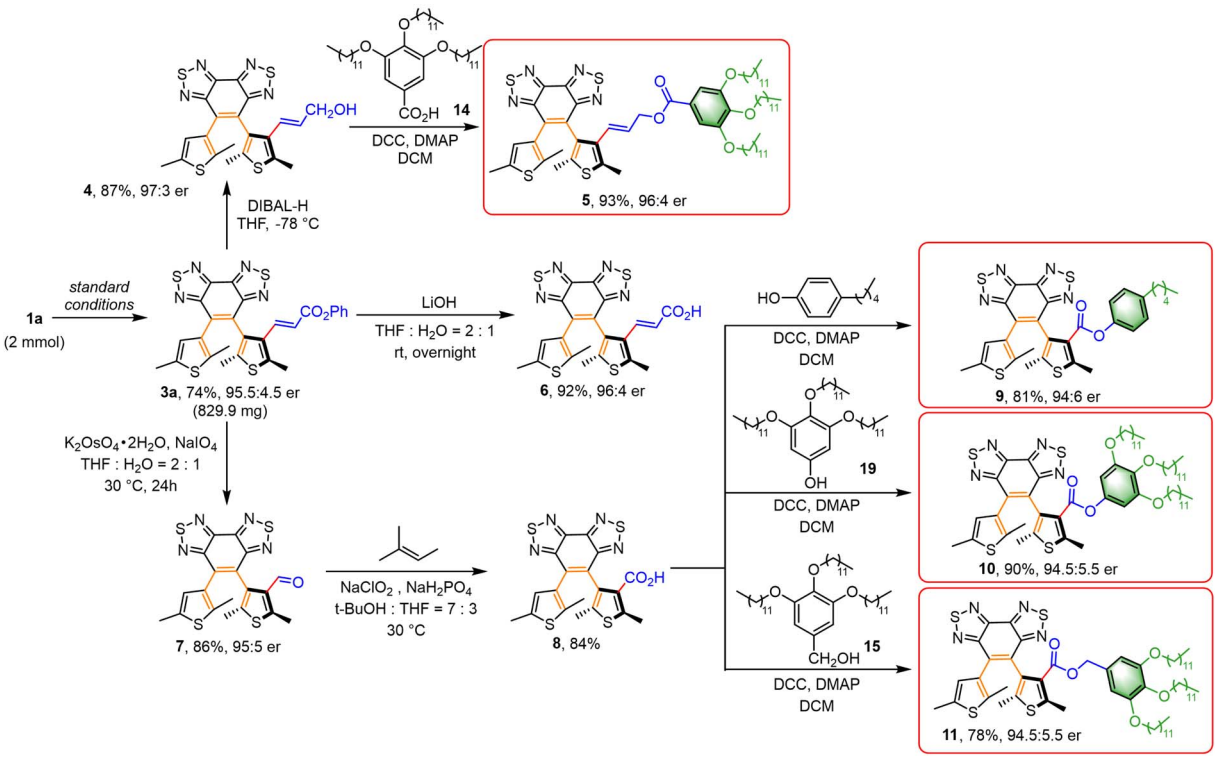

Scheme 2 Scale-up synthesis and further decoration.

crystal X-ray crystallographic analysis (Fig. S1, and Table S3†). Other molecules were assigned by analogy.

Intrinsic chirality and photoswitching behavior

To evaluate the suitability of these derived diarylethenes for photoregulation, we examined their photoswitching characteristics. First, the photoswitching behavior of diarylethene **9** was investigated, which has the simplest molecular structure among the derivatives. Upon exposure to UV light (λ = 313 nm), the ring-open isomer **9o** gradually converted into the corresponding ring-closed isomer **9c** (Fig. 2a). The solution transformed from colorless into orange, along with an increase in absorption at 335–630 nm and a decrease at 290 nm, and reached the photostationary state (PSS) after 5 min (Fig. 2b). Under irradiation with visible light (λ > 490 nm), the solution at the PSS turned back to colorless as a result of the cycloreversion of **9c**. The conversion ratio from **9o** to **9c** (90% in CD_2Cl_2, Fig. 2f; 94% in THF-d8, and S16†) was determined by calculating the peak area ratio of protons in the ^{1}H NMR spectrum of the PSS solution. Compared with the reported intrinsic chiral diarylethenes, the photoswitch **9** is mono-substituted by a mesogenic unit with one rotatable thiophene unit and one unrotatable large bulky aryl group. Therefore, the photoactive anti-parallel conformer **9o–ap** and photoinert parallel conformer **9o–p** (Fig. 2a) can still interconvert into each other in solution. For traditional diarylethenes, this kind of interconversion is typically very fast, thus only average signals appear in their NMR spectra. For **9o**, because the increased steric hindrance reduces the rotation rate of thiophene rings, we can observe both signals of anti-parallel and parallel conformers in the NMR spectra to study the spectral changes based on 1D and 2D NMR. For example, in the structure of **9o–ap**, due to the shielding effect from the facing aryls, the methyl protons (H_e) are in a higher field than those in the *p*-conformer (H_e', Fig. 2h). Similarly, in the structure of **9o–p**, because H_a' is facing the other thiophene ring, it is also in a higher field compared to H_a of **9o–ap**. Considering the complexity of the methyl groups of **9o**, we further checked their chemical shifts using the 2D NOESY spectrum (Fig. S4†). In the structure of **9o–ap**, H_a may have a possible nuclear Overhauser effect (NOE) with nearby H_d and H_e, while for **9o–p**, only H_d' is close to H_a'. As illustrated in the 2D NOESY spectrum, we can distinctly find the coupling signals of H_a with H_d and H_e. Meanwhile, H_c has weak correlations with H_f, which is consistent with the structure of **9o–ap**. In contrast, for **9o–p**, only signals between H_a' and H_d' were observed, suggesting that H_a' is far from H_d' and H_e'. These results can elaborately describe the interconversion between anti-parallel and parallel conformers in the corresponding 1D and 2D NMR. The ratio of **ap**/**p** (43/57 in CD_2Cl_2, 44/56 in THF-d8, Fig. S17†) can be calculated from the peak area ratio of H_a and H_a'. After UV irradiation, signals of these two conformers in ^{1}H NMR both turned into those of **9c** and would recover into two kinds of signals after visible light irradiation. This reversible process can be repeated many times without remarkable degradation (Fig. 2e, and S9†), showing robust fatigue resistance. The thermal stability of **9c** was also found to be excellent, which exhibited only a marginal decrease in absorption over 96 hours at 298 K (Fig. 2d) and 24 hours at 333 K (Fig. S15†). Next, the intrinsic chirality of diarylethene **9**

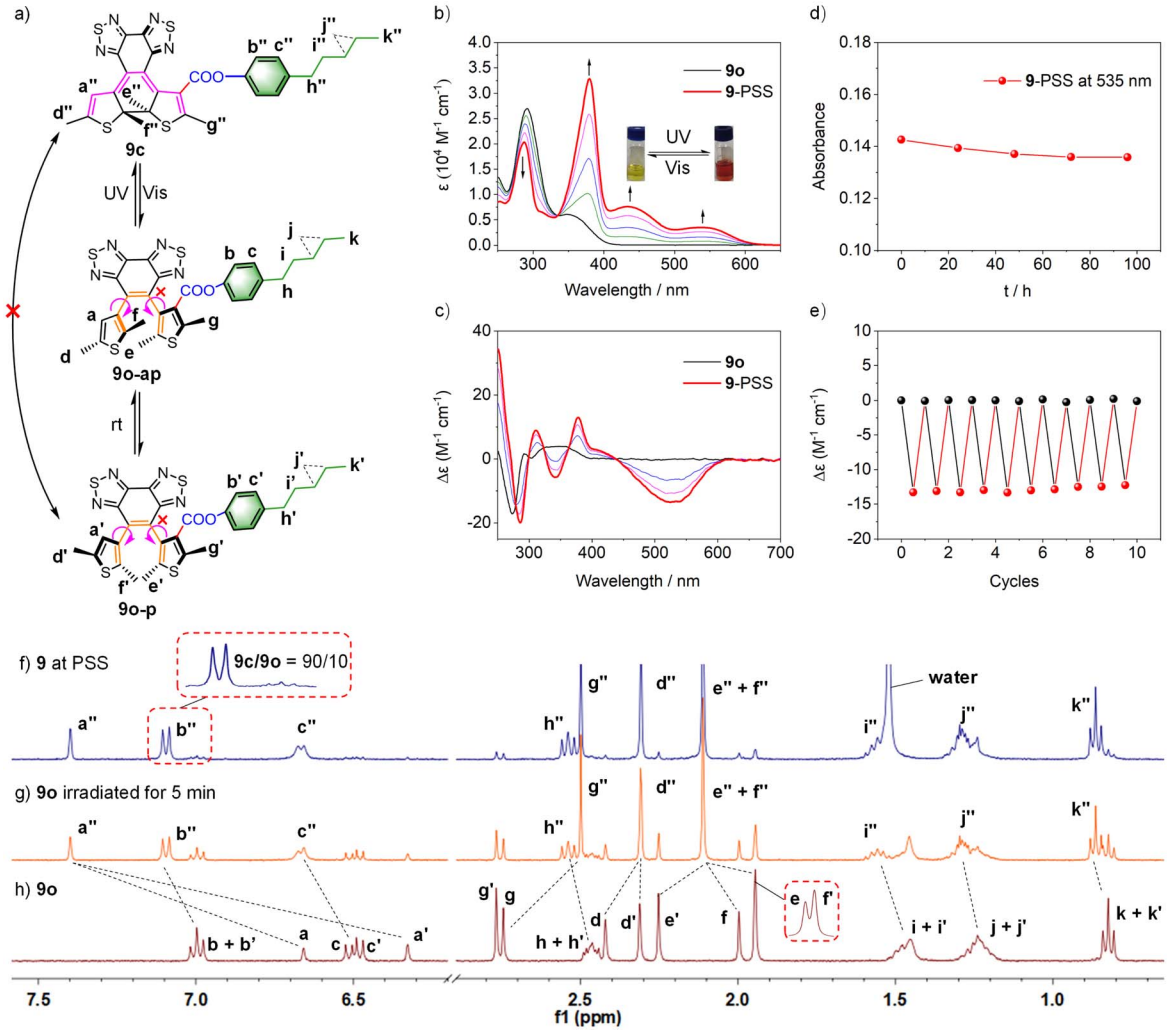

Fig. 2 Photochromic behavior and chiral regulation of **9**. (a) Transformation between the isomers of **9**. (b) Normalized UV-vis spectrum changes ($c = 4 \times 10^{-5}$ M, THF) and (c) CD spectrum changes of **9** ($c = 4 \times 10^{-5}$ M, THF) during irradiation with UV light ($\lambda = 313$ nm). (d) Absorbance changes of **9** at PSS at 535 nm at room temperature for 96 h ($c = 4 \times 10^{-5}$ M, THF). (e) Changes of CD signals of **9** ($c = 4 \times 10^{-5}$ M, THF) at 535 nm during alternative irradiation with UV light ($\lambda = 313$ nm) and visible light ($\lambda > 490$ nm). Irradiation with UV light ($\lambda = 313$ nm) in CD_2Cl_2 ($c = 5 \times 10^{-3}$ M): ^{1}H NMR spectra of (f) **9** at the PSS; (g) **9o** irradiated for 5 min and (h) **9o**.

was further investigated by circular dichroism (CD) spectroscopy. As depicted in Fig. 2c, the ring-open isomer **9o** exhibited a distinct CD peak at 273 nm attributed to Cotton effects, which is uncommon in typical diarylethenes[20] but close to overcrowded alkenes[21] and binaphthyls[22] with axial chirality. Thus, this peak can be attributed to the axial chirality resulting from the substituted thiophene and ethene bridge. Upon irradiation with UV light, distinct signals emerged at 437–612 nm (−) attributed to the formation of ring-closed isomer **9c** with the extending π-conjugation. Meanwhile, a strong peak gradually emerged near 250 nm (+), while the initial peak at 273 nm (−) redshifted to 283 nm (−). These peaks can be attributed to the high asymmetry of **9c** resulting from the cyclohexadiene center and distorted ethene bridge.[10] These observed changes in the overall CD spectrum indicated an enantiospecific transformation of **9** from axial into central chirality. The results of fatigue resistance experiments based on the CD spectrum illustrated that almost no destruction of chirality would occur during the whole transformation (Fig. 2e). As demonstrated, enantioselective olefination can increase the rotation barrier of side aryl groups of sterically hindered diarylethenes, resulting in the steady existence of their chiral enantiomers and achieving specific enantioselectivity at the same time, which can efficiently reduce the dependence on preparative chiral HPLC. Indeed, diarylethene **9** exhibited good photoresponsive properties and chiral regulation ability, which are enough for further photoregulation applications. Additional tests demonstrated that **10** and **11** exhibited comparable performances of photochromism and chiral regulation (Fig. S8–S21, and Table S4†). However, the cycloreversion quantum yields of **10** and **11** exhibited a significant decrease in comparison to **9**, which can be likely ascribed to the large hindrance of the trialkoxyphenyl groups and the non-covalent interactions between the three

dodecane chains and solvent molecules enhancing the hindrance of photocycloreversion.

Photomanipulation of the liquid crystal superstructure

Given the intrinsic chiral photoswitch **9** obtained through enantioselective C–H olefination and decoration with a mesogenic group, we incorporated it into a commercial nematic LC for precise photoregulation of the helical superstructure. The helical twist power (HTP) represents the ability of chiral guest (dopant) compounds to induce a cholesteric liquid crystal (CLC) phase from nematic phases. Chiral photoswitches can effectively utilize their unique optical responsiveness to drive and dynamically adjust the properties of the induced CLCs through the changes of HTP. Thus, we first examined the HTP of **9** by the well-known Cano's method (Fig. S22 and S23†) calculated according to the equation: $\beta_M = (P \cdot c)^{-1}$, where β_M is HTP, P represents the pitch length, and c represents the concentration of the chiral dopant in the LC. Under UV light, the distance between two disclination lines of a mixture comprising **9** and the commercial LC increased from 108.5 to 159.6 μm (Fig. 3c), which is consistent with the decrease of HTP from 69.8 μm^{-1} to 47.4 μm^{-1} (Table S5†), indicating that **9** could effectively twist and manipulate the helical superstructure. Similar tests were conducted with **10** and **11** (Fig. S24, and Table S5†). Unfortunately, **10** and **11** exhibited poorer regulation abilities in the LC possibly due to increased steric hindrance of side groups, resulting in diminished conversion rates. Although this effect may not be apparent in solution (Fig. S18 and S19†), it can become evident in LCs where the movements of molecules are more restricted. Subsequently, compound **9** was mixed with TEB300 and chiral dopant S5011 to prepare a photoresponsive LC system. The reflection color of this LC system can continuously transform from blue into green and then into red under UV light ($\lambda = 365$ nm, 4.0 mW cm^{-2}) irradiation for 20 s (Fig. 3a) accompanied by a redshift of the reflection wavelength from 430 to 650 nm (Fig. 3b), covering the basic RGB colors. Full recovery was achieved by irradiation under visible light ($\lambda = 530$ nm, 1.0 mW cm^{-2}) for 3 min. The reflection bands remained sharp without distinct spectral deformation during the shift process, thus confirming that the photoregulation has negligible destruction on the texture of the LC system attributed to the unique enantiospecific transformation of intrinsic chirality and increased LC compatibility originated from the decorated mesogenic unit. In addition, the color of the LC system remained unchanged after the removal of UV light due to the good thermal stability of **9c**. Next, a patterned image was

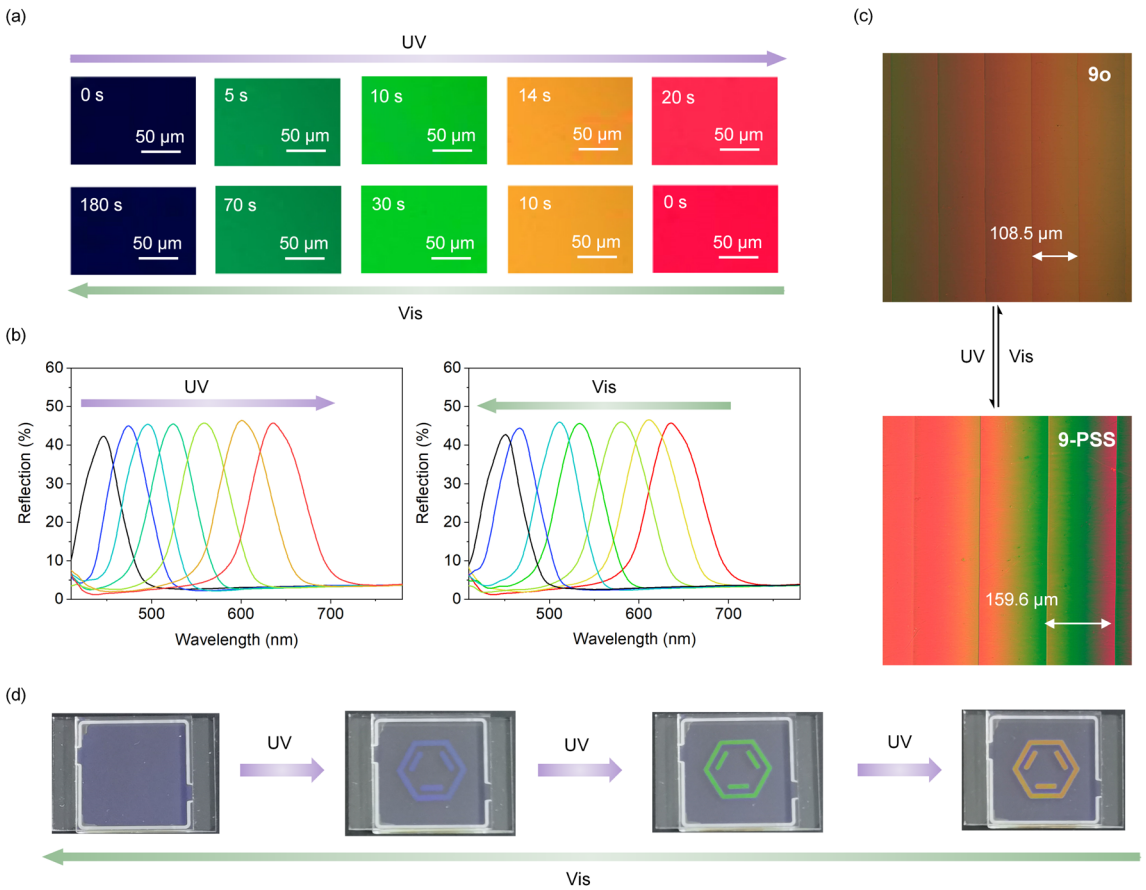

Fig. 3 LC photomanipulation and anti-counterfeiting application. (a) Texture changes of the LC system during photoregulation. (b) Reflection spectra of the LC system during photoregulation. (c) Distance changes between two disclination lines of a mixture of **9** and TEB300. (d) The color changes of the designed pattern.

recorded using light passing through a photomask in the photoresponsive LC system. With the irradiation of UV light, a distinct benzene ring gradually emerged, accompanied by a transition in color passing through blue, green, and orange (Fig. 3d). By precisely controlling the duration of irradiation, it is achievable to maintain the pattern at any intermediate state, without any obvious color migration or blurring of the boundary. This photoresponsive LC system exhibits potential application in the field of anti-counterfeiting.

Conclusions

In conclusion, we proposed a novel strategy to directly construct intrinsic chiral diarylethenes. By employing enantioselective C–H olefination, we successfully synthesized a series of intrinsic chiral diarylethenes with high yields and enantioselectivity. The obtained diarylethenes can be further decorated by incorporating mesogenic units through three-step synthesis for liquid crystal modulation. A photoresponsive liquid crystal system and an anti-counterfeiting method with excellent photoregulatory abilities have been established. Research in the future will primarily concentrate on exploring other applications for these synthesized diarylethenes and further improving their photoregulatory abilities.

Data availability

All data in the manuscript are available in the ESI,† including the experimental details, characterization data, HPLC spectra, and crystallographic data.

Author contributions

G. Z. and X. W. contributed equally to this work. G. Z. and X. W. performed the synthesis and tests and wrote the draft. M. L., W. Z. and B. S. reviewed and edited the manuscript. S. M. and H. L. helped in the experimental process.

Conflicts of interest

There are no conflicts to declare.

Acknowledgements

This work was supported by the National Natural Science Foundation of China (T2488302, 92356301, 22338006, 22108076, 21925109, U22A20388, and 92256302), the National Key R&D Program of China (2022YFA1504302 and 2021YFF0701603), Fundamental Research Funds for the Central Universities (226-2023-00115 and 226-2022-00224), and Zhejiang Provincial NSFC (LD22B030003).

Notes and references

1 (*a*) M. Irie and M. Mohri, *J. Org. Chem.*, 1988, **53**, 803–808; (*b*) S. Takami, S. Kobatake, T. Kawai and M. Irie, *Chem. Lett.*, 2003, **32**, 892–893; (*c*) X. Li, Q. Zou and H. Ågren, *J. Phys. Chem. A*, 2015, **119**, 9140–9147; (*d*) N. M. Wu, H.-L. Wong and V. W.-W. Yam, *Chem. Sci.*, 2017, **8**, 1309–1315.

2 (*a*) H. Jean-Ruel, R. R. Cooney, M. Gao, C. Lu, M. A. Kochman, C. A. Morrison and R. J. D. Miller, *J. Phys. Chem. A*, 2011, **115**, 13158–13168; (*b*) Y. Ishibashi, M. Fujiwara, T. Umesato, H. Saito, S. Kobatake, M. Irie and H. Miyasaka, *J. Phys. Chem. C*, 2011, **115**, 4265–4272; (*c*) Y. Ishibashi, T. Umesato, S. Kobatake, M. Irie and H. Miyasaka, *J. Phys. Chem. C*, 2012, **116**, 4862–4869; (*d*) P. Hong, J. Liu, K.-X. Qin, R. Tian, L.-Y. Peng, Y.-S. Su, Z. Gan, X.-X. Yu, L. Ye, M.-Q. Zhu and C. Li, *Angew. Chem., Int. Ed.*, 2024, **63**, e202316706; (*e*) D. Kolarski, P. Steinbach, C. Bannwarth, K. Klaue and S. Hecht, *Angew. Chem., Int. Ed.*, 2024, **63**, e202318015.

3 (*a*) D. Mendive-Tapia, A. Perrier, M. J. Bearpark, M. A. Robb, B. Lasorne and D. Jacquemin, *Phys. Chem. Chem. Phys.*, 2014, **16**, 18463–18471; (*b*) J. C. H. Chan, W. H. Lam and V. W.-W. Yam, *J. Am. Chem. Soc.*, 2014, **136**, 16994–16997; (*c*) T. Kolmar, S. M. Büllmann, C. Sarter, K. Höfer and A. Jäschke, *Angew. Chem., Int. Ed.*, 2021, **60**, 8164–8173; (*d*) M.-Q. Li, H.-L. Hu, B.-H. Liu, X. Liu, Z.-G. Zheng, H. Tian and W.-H. Zhu, *J. Am. Chem. Soc.*, 2022, **144**, 20773–20784; (*e*) M. Bovoloni, J. Filo, I. Sigmundová, P. Magdolen, Š. Budzák, E. Procházková, M. Tommasini, M. Cigáň and A. Bianco, *Phys. Chem. Chem. Phys.*, 2022, **24**, 23758–23768.

4 (*a*) J.-W. Jiang, P.-S. Zhang, L. Liu, Y.-Q. Li, Y.-B. Zhang, T.-C. Wu, H.-L. Xie, C. H. Zhang, J. X. Cui and J. Chen, *Chem. Eng. J.*, 2021, **425**, 131557; (*b*) Y.-Y. Tang, Y.-L. Zeng and R.-G. Xiong, *J. Am. Chem. Soc.*, 2022, **144**, 8633–8640; (*c*) M. Karmakar, S. K. Bag, B. Mondal and A. Thakur, *J. Mater. Chem. C*, 2022, **10**, 8860–8873.

5 (*a*) S. Pullen, J. Tessarolo and G. H. Clever, *Chem. Sci.*, 2021, **12**, 7269–7293; (*b*) T. Fukushima, K. Tamaki, A. Isobe, T. Hirose, N. Shimizu, H. Takagi, R. Haruki, S.-I. Adachi, M. J. Hollamby and S. Yagai, *J. Am. Chem. Soc.*, 2021, **143**, 5845–5854; (*c*) B. H. Tang, M. Pauls, C. Bannwarth and S. Hecht, *J. Am. Chem. Soc.*, 2024, **146**, 45–50; (*d*) M. Li, L.-J. Chen, Z. P. Zhang, Q. F. Luo, H.-B. Yang, H. Tian and W.-H. Zhu, *Chem. Sci.*, 2019, **10**, 4896–4904; (*e*) W.-L. Zhou, X.-Y. Dai, W.-J. Lin, Y. Chen and Y. Liu, *Chem. Sci.*, 2023, **14**, 6457–6466.

6 (*a*) L. Gu, L.-J. Zhang, X. Luo, Y. Zheng, Z.-W. Ye, M. Lv, J.-Q. Chen, C.-L. Chen, Y. Xiao, W.-H. Zhu, X.-H. Qian and Y.-J. Yang, *Sci. China: Chem.*, 2021, **64**, 253–262; (*b*) C. Li, K. Xiong, Y. Chen, C. Fan, Y.-L. Wang, H. Ye and M.-Q. Zhu, *ACS Appl. Mater. Interfaces*, 2020, **12**, 27651–27662; (*c*) H. Yang, M. Li, C. Li, Q. Luo, M.-Q. Zhu, H. Tian and W.-H. Zhu, *Angew. Chem., Int. Ed.*, 2020, **59**, 8560–8570.

7 (*a*) J. X. Hou, J. H. Wang, A. Ryabchun and B. L. Feringa, *Adv. Funct. Mater.*, 2024, 2312831; (*b*) Y. Cai, Z. Guo, J. Chen, W. Li, L. Zhong, Y. Gao, L. Jiang, L. Chi, H. Tian and W.-H. Zhu, *J. Am. Chem. Soc.*, 2016, **138**, 2219–2224; (*c*) M. Li, L.-J. Chen, Y. Cai, Q. Luo, W. Li, H.-B. Yang, H. Tian and W.-H. Zhu, *Chem*, 2019, **5**, 634–648; (*d*) Y. Wu, Y. R. Ren, X.-X. Zeng, H.-L. Hu, M.-Q. Li, J.-Z. Li, T.-C. He, X.-S. Li, Z.-Q. Yu and W.-H. Zhu, *Smart Mol.*, 2023, **1**, e20230003.

8 (*a*) T. Yamaguchi, T. Inagawa, H. Nakazumi, S. Irie and M. Irie, *Chem. Mater.*, 2000, **12**, 869–871; (*b*) Y.-N. Li and Q. Li, *Org. Lett.*, 2012, **14**, 4362–4365; (*c*) Y. Li, M. Wang, A. Urbas and L. Quan, *J. Mater. Chem. C*, 2013, **1**, 3917–3923; (*d*) Z.-G. Zheng, H.-L. Hu, Z.-P. Zhang, B.-H. Liu, M.-Q. Li, D.-H. Qu, H. Tian, W.-H. Zhu and B. L. Feringa, *Nat. Photonics*, 2022, **16**, 226–234; (*e*) H.-L. Hu, M. He, X.-S. Liang, M.-Q. Li, C. L. Yuan, B.-H. Liu, X. Liu, Z. G. Zheng and W.-H. Zhu, *Matter*, 2023, **6**, 3927–3939.

9 (*a*) M. Irie, T. Fukaminato, K. Matsuda and S. Kobatake, *Chem. Rev.*, 2014, **114**, 12174–12277; (*b*) S.-M. Guo, M.-Q. Li, H.-L. Hu, T. Xu, H.-C. Xi and W.-H. Zhu, *Chem. Sci.*, 2023, **14**, 6237–6243.

10 (*a*) W.-L. Li, C.-H. Jiao, Y.-S. Xie, K. Nakatani, H. Tian and W.-H. Zhu, *Angew. Chem., Int. Ed.*, 2014, **53**, 4603–4607; (*b*) W.-L. Li, X. Li, Y.-S. Xie, Y. Wu, M. Q. Li, X. Y. Wu, W. H. Zhu and H. Tian, *Sci. Rep.*, 2015, **5**, 9186.

11 (*a*) P. W. N. M. van Leeuwen, P. C. J. Kamer, C. Claver, O. Pamies and M. Dieguez, *Chem. Rev.*, 2011, **111**, 2077–2118; (*b*) R. Connon, B. Roche, B. V. Rokade and P. J. Guiry, *Chem. Rev.*, 2021, **121**, 6373–6521; (*c*) C. X. Liu, S. Y. Yin, F. N. Zhao, H. Yang, Z. L. J. Feng, Q. Gu and S. L. You, *Chem. Rev.*, 2023, **123**, 10079–10134; (*d*) D.-B. Zhao and K.-L. Ding, *ACS Catal.*, 2013, **3**, 928–944; (*e*) G.-Q. Yang and W.-B. Zhang, *Chem. Soc. Rev.*, 2018, **47**, 1783–1810.

12 (*a*) T. K. Achar, S. Maiti, S. Jana and D. Maiti, *ACS Catal.*, 2020, **10**, 13748–13793; (*b*) G. Liao, T. Zhou, Q.-J. Yao and B.-F. Shi, *Chem. Commun.*, 2019, **55**, 8514–8523; (*c*) J. A. Carmona, C. Rodríguez-Franco, R. Fernández, V. Hornillos and J. M. Lassaletta, *Chem. Soc. Rev.*, 2021, **50**, 2968–2983; (*d*) J. K. Cheng, S.-H. Xiang, S.-Y. Li, L. Ye and B. Tan, *Chem. Rev.*, 2021, **121**, 4805–4902; (*e*) C.-X. Liu, W. W. Zhang, S. Y. Yin and S. L. You, *J. Am. Chem. Soc.*, 2021, **143**(35), 14025–14040.

13 W. H. Zhu, Y. H. Yang, R. Métivier, Q. Zhang, R. Guillot, Y.-S. Xie, H. Tian and K. Nakatani, *Angew. Chem., Int. Ed.*, 2011, **50**, 10986–10990.

14 W.-L. Li, Y.-S. Cai, X. Li, H. Ågren, H. Tian and W.-H. Zhu, *J. Mater. Chem. C*, 2015, **3**, 8665–8674.

15 Y. Zhao and D. G. Truhlar, *Theor. Chem. Acc.*, 2008, **120**, 215–241.

16 (*a*) J. Guo, H. He, Z. Ye, K. Zhu, Y. Wu and F. Zhang, *Org. Lett.*, 2018, **20**, 5692–5695; (*b*) C. Y. He, C. Z. Wu, F. L. Qing and X. Zhang, *J. Org. Chem.*, 2014, **79**, 1712–1718; (*c*) H. He, J. Guo, W. Sun, B. Yang, F. Zhang and G. Liang, *J. Org. Chem.*, 2020, **85**, 3788–3798; (*d*) J. Zhang, W. Chen, A. J. Rojas, E. V. Jucov, T. V. Timofeeva, T. C. Parker, S. Barlow and S. R. Marder, *J. Am. Chem. Soc.*, 2013, **135**, 16376–16379.

17 (*a*) J. Luo, T. Zhang, L. Wang, G. Liao, Q.-J. Yao, Y.-J. Wu, B.-B. Zhan, Y. Lan, X.-F. Lin and B.-F. Shi, *Angew. Chem., Int. Ed.*, 2019, **58**, 6708–6712; (*b*) Q.-J. Yao, S. Zhang, B.-B. Zhan and B.-F. Shi, *Angew. Chem., Int. Ed.*, 2017, **56**, 6617–6621; (*c*) L. Jin, Q.-J. Yao, P.-P. Xie, Y. Li, B. B. Zhan, Y. Q. Han, X. Hong and B.-F. Shi, *Chem*, 2020, **6**, 497–511; (*d*) Q.-J. Yao, P.-P. Xie, Y.-J. Wu, Y.-L. Feng, M.-Y. Teng, X. Hong and B.-F. Shi, *J. Am. Chem. Soc.*, 2020, **142**, 18266–18276; (*e*) J. Zheng, W.-J. Cui, C. Zheng and S.-L. You, *J. Am. Chem. Soc.*, 2016, **138**, 5242–5245; (*f*) Y. J. Li, Y.-C. Liou, X.-R. Chen and L. Ackermann, *Chem. Sci.*, 2022, **13**, 4088–4094; (*g*) W. Ali, G. Prakash and D. Maiti, *Chem. Sci.*, 2021, **12**, 2735–2759; (*h*) Z. Dong, J. Li, T. Yao and C. Zhao, *Angew. Chem., Int. Ed.*, 2023, **62**, e202315603.

18 (*a*) B.-B. Zhan, L. Wang, J. Luo, X. F. Lin and B. F. Shi, *Angew. Chem., Int. Ed.*, 2020, **59**, 3568–3572; (*b*) L. Jin, P. Zhang, Y. Li, X. Yu and B. F. Shi, *J. Am. Chem. Soc.*, 2021, **143**, 12335–12344; (*c*) G. Liao, T. Zhang, L. Jin, B. J. Wang, C. K. Xu, Y. Lan, Y. Zhao and B. F. Shi, *Angew. Chem., Int. Ed.*, 2022, **61**, e202115221.

19 (*a*) A. Ryabchun, Q. Li, F. Lancia, I. Aprahamian and N. Katsonis, *J. Am. Chem. Soc.*, 2019, **141**, 1196–1200; (*b*) Y. Zhan, S. Calierno, J. Peixoto, L. Mitzer, D. J. Broer and D. Liu, *Angew. Chem., Int. Ed.*, 2022, **61**, e202207468; (*c*) W. Kang, Y. Tang, X. Meng, S. Lin, X. Zhang, J. Guo and Q. Li, *Angew. Chem., Int. Ed.*, 2023, **62**, e202311486; (*d*) J. Hou, R. Toyoda, S. C. J. Meskers and B. L. Feringa, *Angew. Chem., Int. Ed.*, 2022, **61**, e202206310.

20 (*a*) T. Nakashima, K. Yamamoto, Y. Kimura and T. Kawai, *Chem.–Eur. J.*, 2013, **19**, 16972–16980; (*b*) H. Jin-nouchi and M. Takeshita, *Chem.–Eur. J.*, 2012, **18**, 9638–9644.

21 (*a*) B. L. Feringa, *Acc. Chem. Res.*, 2001, **34**, 504–513; (*b*) D. Zhao, T. M. Neubauer and B. L. Feringa, *Nat. Commun.*, 2015, **6**, 6652–6658.

22 (*a*) C. Gao, S. Silvi, X. Ma, H. Tian, A. Credi and M. Venturi, *Chem.–Eur. J.*, 2012, **18**, 16911–16921; (*b*) C. Gütz, R. Hovorka, C. Klein, Q.-Q. Jiang, C. Bannwarth, M. Engeser, C. Schmuck, W. Assenmacher, W. Mader, F. Topić, K. Rissanen, S. Grimme and A. Lützen, *Angew. Chem., Int. Ed.*, 2014, **53**, 1693–1698.